

Don't Start From Scratch: Leveraging Prior Data to Automate Robotic Reinforcement Learning

Homer Walke^{*1}, Jonathan Yang¹, Albert Yu², Aviral Kumar¹, Jędrzej Orbik¹, Avi Singh³, and Sergey Levine^{1,3}

¹UC Berkeley ²UT Austin ³Google

Abstract: Reinforcement learning (RL) algorithms hold the promise of enabling autonomous skill acquisition for robotic systems. However, in practice, real-world robotic RL typically requires time consuming data collection and frequent human intervention to reset the environment. Moreover, robotic policies learned with RL often fail when deployed beyond the carefully controlled setting in which they were learned. In this work, we study how these challenges can all be tackled by effective utilization of diverse offline datasets collected from previously seen tasks. When faced with a new task, our system adapts previously learned skills to quickly learn to both perform the new task *and* return the environment to an initial state, effectively performing its own environment reset. Our empirical results demonstrate that incorporating prior data into robotic reinforcement learning enables autonomous learning, substantially improves sample-efficiency of learning, and enables better generalization. Project website: <https://sites.google.com/view/ariel-berkeley/>

Keywords: autonomous RL, offline RL, reset-free manipulation

1 Introduction

Reinforcement learning (RL) provides a general learning-based framework that, in principle, could be utilized to acquire any goal-directed behavior. However, in practice, the standard RL formulation overlooks many of the challenges that arise in real-world robotic learning. RL problems are classically (though not exclusively) situated in settings where ample exploration can be performed from scratch, the environment can be reset episodically, and the focus is more on attaining the highest possible performance rather than good generalization, such as in the case of playing a video game. Real-world robotic learning problems have very different constraints. With real-world robots, online interaction and exploration are often at a premium, the robot must figure out how to reset the environment itself between attempts, and the natural variability and uncertainty of the real world makes generalization far more essential than squeezing out every bit of final performance.

Humans and animals handle each of these challenges in the real world. However, in contrast to standard robotic RL settings, humans do not approach each new problem with a blank slate: we leverage prior experience to help us acquire new skills quickly, scaffold the process of learning that skill (e.g., by using our existing skills to practice and try again), and utilize representations learned from prior experience to ensure that the new skill is represented in a robust and generalizable way. We study an analogous approach in this work and propose a complete system for extracting useful skills from prior data and applying them to learn new tasks autonomously. Although the individual components of our system are based on previously proposed principles and methods for offline RL [1], multi-task learning with task embeddings [2, 3], and reset-free learning with forward-backward controllers [4, 5, 6, 7, 8], our system combines these components into a novel framework that effectively enables real-world robotic learning and leverages prior data for all of these parts.

Our system consists of two phases: offline learning using the prior data, and mostly autonomous online fine-tuning on a new task (see Figure 1), where only occasional resets are provided. In the

^{*}homer_walke@berkeley.edu

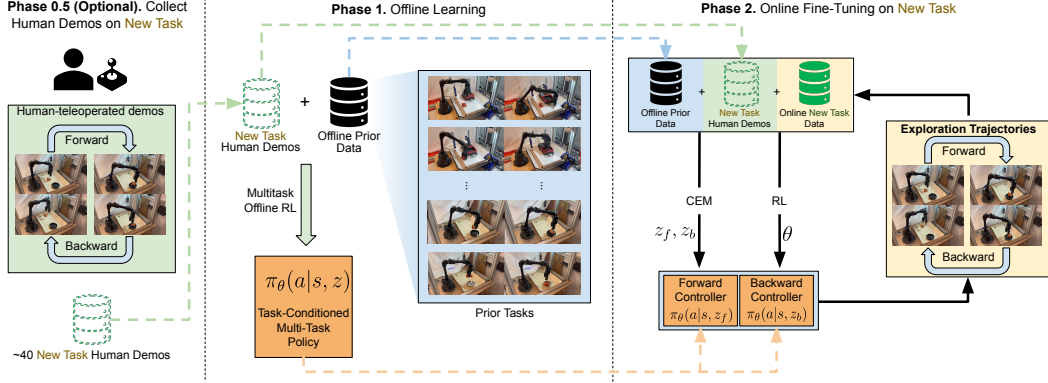


Figure 1: **Overview of our system.** In the offline phase (middle), we train a multi-task policy that captures prior knowledge from an offline dataset of previously experienced tasks and, optionally, a handful of human-teleoperated demos of a new task (left). Then in the online phase (right) the multi-task policy is used to initialize both a forward policy and a backward (reset) skill for learning the new task, improving learning speed and generalization.

offline phase, we use offline RL to extract skills and representations from the prior data. Then, in the online phase, we adapt the learned skills to the new task, alternating between attempting the task and resetting the environment. If the behaviors required to perform the new task and reset the environment are structurally similar to those in the prior data, the skills learned offline will succeed with non-negligible probability, providing a learning signal that allows the agent to adapt its behavior with only a small amount of online data. Moreover, where policies learned from narrow data may overfit to unimportant details of the environment and fail when those details change, policies learned from diverse multi-task data can generalize to new conditions with little to no adaptation.

Our main contribution is demonstrating that incorporating prior data into a reinforcement learning system simultaneously addresses several key challenges in real-world robotic RL: sample-efficiency, zero-shot generalization, and autonomous non-episodic learning. We validate our approach on real-world robotic manipulation, where we show that our method makes it possible to learn new manipulation skills via RL in settings where prior approaches struggle to make progress, reach final performance that is comparable to what the algorithm can attain when provided with “oracle” demonstration data for the new task, and acquire policies that generalize more broadly than those trained only on single-task data.

2 Related Work

Prior work has explored learning behaviors from offline datasets, leveraging multi-task data, and reinforcement learning with minimal resets. We build on techniques from each area to devise a complete system for automated robot learning. We briefly review some related works below.

Accelerating online RL with offline data. We use an offline RL method [9, 10, 11, 12, 13, 14, 15, 16, 1, 17, 18, 19] to extract useful skills and representations from prior data, but our system includes additional components that allow us to use multi-task offline data and autonomously fine-tune the policy online by learning to both perform the task and reset.

Multi-task RL. Similar to methods for multi-task RL [20, 21, 22, 23, 24, 25, 26, 27, 28, 2, 29, 3], we adopt the strategy learning a single policy conditional on a space of tasks. However unlike multi-task RL methods, our focus is adapting this multi-task policy to unseen tasks. Perhaps the closest prior system to ours is MT-Opt [2], which addresses multi-task learning for a similar class of pick-and-place robotic manipulation tasks. However, in contrast to this prior work, our focus is not on how to train a multi-task policy, but specifically on how prior offline data from varied tasks can be leveraged to improve the autonomy and generalization when learning a new task. While Kalashnikov et al. [2] also evaluates fine-tuning to new tasks, our system goes significantly further, aiming to automate resets (which the prior work does not address, instead using an instrumented bin setup), and evaluating the benefits in terms of generalization and efficiency for the new task.

Reset-free RL. Our system aims to utilize prior data to autonomously learn robotic skills, leveraging prior experience to both accelerate the learning of a new behavior and the process of learning how to

reset between attempts. Prior work has tackled this “reset-free” learning problem [30] in a number of ways. Some prior work uses a curriculum-based approach, which relies on the observation that when learning several tasks simultaneously, some tasks reset others, thus forming a curriculum [31, 32, 33, 4, 34]. While Gupta et al. [31] also uses a multi-task setup to automate resets, this prior paper involves a small number of tasks that all focus on enabling reset-free learning for a particular (single) skill, whereas our focus is specifically on using prior data for *other* tasks to enable a *new* task to be learned as autonomously as possible. Other approaches learn separate controllers for performing the task and resetting the environment [4, 5, 6, 7, 8]. Though our method also learns separate controllers, we initialize them with potentially useful skills extracted from prior data. Most similar to our work, Sharma et al. [8] use prior data in the form of demonstrations to accelerate learning forward and reset behaviors. Our system can use expert demonstrations of the target task, but our main focus is using potentially sub-optimal data from other tasks.

3 Preliminaries

The goal in RL is to learn a policy $\pi(\mathbf{a}|\mathbf{s})$ that maximizes the long-term cumulative discounted reward in a Markov decision process (MDP), which is defined as a tuple $\mathcal{M} := (\mathcal{S}, \mathcal{A}, P, r, \rho, \gamma)$, with state space \mathcal{S} , action space \mathcal{A} , transition function $P : \mathcal{S} \times \mathcal{A} \rightarrow \Delta(\mathcal{S})$, reward function $r : \mathcal{S} \times \mathcal{A} \rightarrow \mathbb{R}$, initial state distribution $\rho \in \Delta(\mathcal{S})$, and discount factor $\gamma \in [0, 1]$. The objective is to optimize the policy against the cumulative discounted return objective: $J(\pi) := \mathbb{E} [\sum_i \gamma^i r(\mathbf{s}_i, \mathbf{a}_i)]$. The Q-function $Q^\pi(\mathbf{s}, \mathbf{a})$ for a policy $\pi(\mathbf{a}|\mathbf{s})$ is the long-term discounted return obtained by executing action \mathbf{a} at state \mathbf{s} and following $\pi(\mathbf{a}|\mathbf{s})$ thereafter. $Q^\pi(\mathbf{s}, \mathbf{a})$ is the fixed point of $Q(\mathbf{s}, \mathbf{a}) := R(\mathbf{s}, \mathbf{a}) + \gamma \mathbb{E}_{\mathbf{s}' \sim P(\cdot|\mathbf{s}, \mathbf{a}), \mathbf{a}' \sim \pi(\cdot|\mathbf{s}')} [Q(\mathbf{s}', \mathbf{a}')]]$, which is known as the Bellman equation. While the standard RL objective can be optimized in several ways, in this work we build on the class of actor-critic methods [35, 36, 19]. A typical actor-critic method alternates between two phases: policy evaluation and policy improvement. In policy evaluation, the current policy $\pi(\mathbf{a}|\mathbf{s})$ is evaluated by fitting an action-value function $Q^\pi(\mathbf{s}, \mathbf{a})$. In policy improvement, the policy or actor $\pi(\mathbf{a}|\mathbf{s})$ is updated to maximize the expected Q-value.

4 Autonomous Robotic Reinforcement Learning with Prior Data

First, we formalize our problem statement and describe our evaluation setup. Our goal is to utilize data from previous tasks to address three key challenges in robotic reinforcement learning: sample-efficiency, autonomous learning, and generalization and robustness to unseen test conditions. We assume access to a prior dataset $\mathcal{D}_{\text{prior}}$ of experience collected from multiple training tasks: $\mathcal{D}_{\text{prior}} = \bigcup_{j=1}^N \mathcal{D}_j$ where $\mathcal{D}_j = \{(\mathbf{s}_i^j, \mathbf{a}_i^j, \mathbf{s}_i^j, r_i^j)\}_{i=1}^K$ denotes the chunk of the prior data corresponding to task τ_j . Our goal will be to extract a rich repertoire of skills from this diverse, multi-task prior dataset $\mathcal{D}_{\text{prior}}$ to quickly solve a new target task τ^* . For the prior data to be useful, the training tasks must share structural similarity with the new task. We evaluate two settings, based on the level of similarity between the tasks in $\mathcal{D}_{\text{prior}}$ and τ^* . In the first setting, which we call **direct transfer**, τ^* is not seen at all during training. For direct transfer to succeed, the training tasks must share enough similarity with the target task that a policy trained on $\mathcal{D}_{\text{prior}}$ achieves a non-zero success rate on τ^* . If this condition does not hold, we evaluate in a second setting which we call **transfer with demonstrations**. We provide additional guidance by augmenting $\mathcal{D}_{\text{prior}}$ with a small number of demonstrations of the target task \mathcal{D}_{τ^*} (collected by human teleoperation) so that $\mathcal{D}_{\text{prior}} = \mathcal{D}_{\text{prior}} \cup \mathcal{D}_{\tau^*}$. (This is labeled as an optional Stage 0.5 in Fig. 1.) In both settings, when the robot is practicing on the target task τ^* , it is provided with minimal external resets, in accordance with the autonomous RL paradigm [30]. The learned agent is then evaluated on the same task τ^* , but this time the environment is reset after every episode.

Our method, which we call Autonomous RobotIc REinforcement Learning (ARIEL), consists of two phases: offline learning using the prior data followed by mostly autonomous online adaptation to a target task (see Figure 1).

4.1 Learning From Prior Data with Offline RL

Given a dataset from previous tasks, we first aim to extract skills and representations that could be useful for learning downstream tasks. The multi-task dataset $\mathcal{D}_{\text{prior}}$ can come from many different sources: human demonstrations, sub-optimal data from previous reinforcement learning experiments, or even data collected using (imperfect) hand-engineered policies. To make use of this multi-task dataset for downstream tasks, we train a conditional policy $\pi_\theta(\mathbf{a}|\mathbf{s}, \mathbf{z})$ using offline RL;

we utilize the AWAC [1] algorithm in our experiments. This policy is conditioned on a task index \mathbf{z} (represented as a one-hot vector) that informs the agent which task it is performing. Training a single multi-task policy offers several advantages over training separate policies on the prior dataset. First, we are able to learn a representation of policy inputs and outputs (in this case, images and desired change in end-effector pose, respectively) which is shared across tasks, and is therefore more likely to generalize well when faced with new inputs: both through interpolation (if the new task is similar to previously seen tasks), and extrapolation (for novel tasks). Second, when attempting a new task, we only need to sample actions from a single pre-trained policy, as opposed to choosing from an ensemble of pre-trained policies. Finally, this also allows our method to gracefully scale with the number of tasks in the prior dataset. After the offline learning phase, we have a multi-task policy $\pi_\theta(\mathbf{a}|\mathbf{s}, \mathbf{z})$ that can perform each of the tasks in the prior data. In Section 5 we discuss the specific tasks we use in our prior data and how we generate the prior dataset for our experiments.

4.2 Autonomous Online Training

After extracting skills from the offline data, our systems adapts the skills to efficiently learn a new task with minimal externally provided environment resets. Since the environment is not frequently reset, the agent must simultaneously learn to perform the task and reset the environment to the initial state so it can continue practicing. Prior work has tackled this problem by learning distinct forward and backward controllers, alternating between applying the forward controller to perform the task and applying the backward controller to reset the task [4, 5, 6, 7, 8]. We adopt an analogous strategy, but we leverage the multi-task policy described in the previous section to bootstrap learning in both the forward and backward direction, which both helps to overcome the exploration challenge and provide automated resets more quickly than if the backward controller were trained from scratch.

To enable this, we fine-tune the parameters of the policy $\pi_\theta(\mathbf{a}|\mathbf{s}, \mathbf{z})$ obtained after the offline phase with online data from the new task τ^* , which we denote as \mathcal{D}_{τ^*} , similarly to prior work that uses online fine-tuning to improve upon policies learned via offline RL alone [1]. However, since we have a multi-task policy, we must confront the question of which skill(s), parameterized by task indices \mathbf{z} , should be chosen to start fine-tuning for the forward and backward controller. If demonstrations of the target task were provided (in the transfer with demonstrations setting), we can use the task indices associated with these demonstrations. Otherwise, if no demonstrations were provided (the direct transfer setting), we must automatically determine which prior skill (or combination of prior skills) to fine-tune. To do this, we treat the task index \mathbf{z} as a continuous, learnable parameter and use data collected during online reinforcement learning to select the \mathbf{z} 's best suited for the given new task. In this sense, we treat \mathbf{z} as a task embedding [3] that is automatically adapted for the task at hand, similar to prior work in meta-reinforcement learning [37].

Since we aim to learn both a forward and backward controller, we optimize for two skills, parameterized by two distinct task embeddings \mathbf{z}_f and \mathbf{z}_b , that respectively perform the task and reset the environment. Conditioning the policy on \mathbf{z}_f results in the forward controller $\pi_\theta(\mathbf{a}|\mathbf{s}, \mathbf{z}_f)$ that performs the task, whereas conditioning the policy on \mathbf{z}_b results in the backward controller $\pi_\theta(\mathbf{a}|\mathbf{s}, \mathbf{z}_b)$ that resets the environment according to the initial state distribution of the task τ^* . During fine-tuning we alternate between applying the forward controller and backward controller, optimizing the forward controller with rewards for completing the task $r_f(\mathbf{s}, \mathbf{a})$ and the backward controller with rewards for returning to the initial state distribution $r_b(\mathbf{s}, \mathbf{a})$. We optimize the parameters \mathbf{z}_f and \mathbf{z}_b in tandem with the policy and value function parameters θ and ϕ . The parameters of the policy and value function are updated using using an actor-critic algorithm (we use AWAC [1]). The embeddings \mathbf{z}_f and \mathbf{z}_b are optimized differently, as we discuss next.

Optimizing task embeddings \mathbf{z}_f and \mathbf{z}_b . Since our goal is to learn the target task τ^* as quickly as possible, and with minimal resets, we need to effectively explore the environment during online training. An ideal approach that explores effectively must not prematurely commit to a particular value of \mathbf{z}_f and \mathbf{z}_b until the online experience clearly indicates so, and at the same time, it should be fast at collapsing to the correct values of \mathbf{z}_f and \mathbf{z}_b , when it is apparent from the online experience gathered until then. We found that the cross-entropy method (CEM) [38] provided us with a favorable balance between exploration and exploitation. CEM provides a way to initialize the task embedding to a *distribution*, which ensures that we do not have to commit to fine-tuning any one particular skill. Since we want to optimize both the forward and backward embeddings \mathbf{z}_f and \mathbf{z}_b , we fit two sampling distributions with CEM, $q_f(\mathbf{z})$ and $q_b(\mathbf{z})$. The distribution of tasks in the prior data $\mathcal{D}_{\text{prior}}$ provides us with a natural (and hopefully informative) prior to initialize $q_f(\mathbf{z})$ and $q_b(\mathbf{z})$. On each iteration of training, we sample a \mathbf{z} from either $q_f(\mathbf{z})$ or $q_b(\mathbf{z})$ and roll out the policy con-

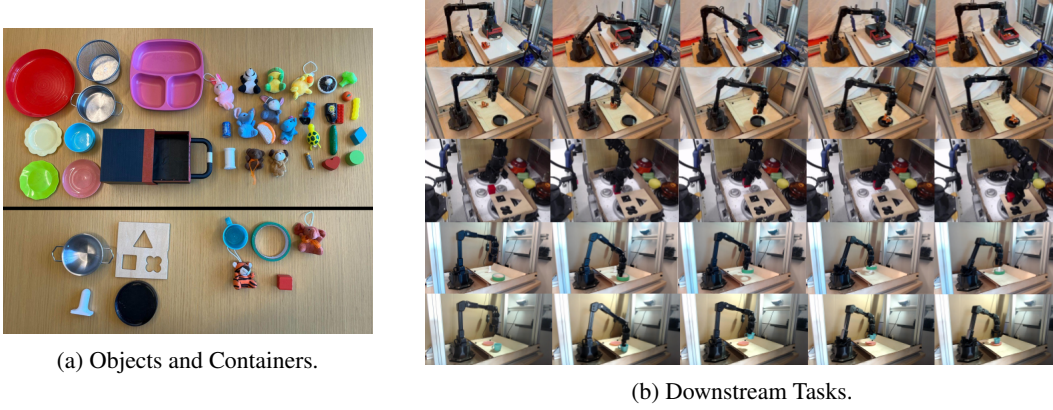


Figure 2: **(a):** Objects used to construct the train tasks (upper) and test tasks (lower) in our experiments. **(b):** Selected test tasks on our real-world robotic setup.

ditioned on this \mathbf{z} value for M steps. These M -step trajectories essentially correspond to an episode in episodic RL, however the environment is (typically) not reset afterward. We alternate between sampling the \mathbf{z} from $q_f(\mathbf{z})$ or $q_b(\mathbf{z})$ to alternate between applying the forward and reset controllers. The reward function correspondingly alternates between $r_f(\mathbf{s}, \mathbf{a})$ and $r_b(\mathbf{s}, \mathbf{a})$. We periodically refit $q_f(\mathbf{z})$ and $q_b(\mathbf{z})$ to the J most recently sampled \mathbf{z} 's that resulted in trajectories that successfully completed or reset the task, respectively. We update the policy and value function parameters θ and ϕ using the update steps from an RL algorithm as summarized in Algorithm 1. Every N steps, we provide an external reset to the environment. However, $N \gg M$, so the external resets are infrequent. For example, in one of our real world tasks, $M = 20$, and $N = 400$. In theory, we could run our method without any manual resets at all, but we found a small number of manual resets necessary to recover from certain states, similarly to prior work on reset-free RL [5].

4.3 Algorithm Summary

Algorithm 1 ARIEL online adaptation

Input: pre-trained policy $\pi_\theta(\mathbf{a}|\mathbf{s}, \mathbf{z})$, Q-function $Q_\phi^\pi(\mathbf{s}, \mathbf{a}, \mathbf{z})$

```

1: Initialize buffer  $\mathcal{B}$ , CEM models  $q_f, q_b$ 
2: Fit  $q_f(\mathbf{z})$  and  $q_b(\mathbf{z})$  to offline task indices
3:  $d \leftarrow f$  // task direction, f is forward, b is backward
4: while not done do
5:    $\mathbf{s} \sim \rho(\mathbf{s}_0)$  // sample initial state (i.e external reset)
6:   for  $N$  steps do
7:     // sample new task embedding at max trajectory length
8:     if steps %  $M == 0$  then
9:        $\mathbf{z} \sim q_d$ 
10:    end if
11:    Sample  $\mathbf{a} \sim \pi(\cdot|\mathbf{s}, \mathbf{z})$ , observe  $\mathbf{s}' \sim p(\cdot|\mathbf{s}, \mathbf{a})$ 
12:     $\mathcal{B} \leftarrow \mathcal{B} \cup \{(\mathbf{s}, \mathbf{a}, r_d(\mathbf{s}', \mathbf{a}), \mathbf{s}', \mathbf{z})\}$ 
13:    if  $r_d(\mathbf{s}', \mathbf{a})$  then
14:       $\text{switch}(d)$  // switch task direction
15:    end if
16:    update  $\pi_\theta, Q_\phi^\pi$  w/ RL, update  $q_f(\mathbf{z}), q_b(\mathbf{z})$  w/ CEM
17:     $\mathbf{s} \leftarrow \mathbf{s}'$ 
18:  end for
19: end while

```

To summarize, we first use offline RL on $\mathcal{D}_{\text{prior}}$ to obtain a multi-task policy $\pi_\theta(\mathbf{a}|\mathbf{s}, \mathbf{z})$ and value function $Q_\phi(\mathbf{s}, \mathbf{a}, \mathbf{z})$. Then, in the online phase (see Algorithm 1), we adapt this policy and value function to a target task. Notably, the offline phase occurs only once, but the online phase can be run many times to efficiently learn many new tasks. During online adaptation, we use $\pi_\theta(\mathbf{a}|\mathbf{s}, \mathbf{z})$ to initialize a forward and backward controller that perform and reset the task respectively. Alternating between applying the forward and backward controller allows the agent to autonomously practice the target task. Our system enables us to learn the new task efficiently and with minimal environment resets by leveraging prior data from previous tasks. We provide further implementation details in the Appendix.

5 Experiment Setup

We now describe our experimental setup for data collection, training, and evaluation.

Robotic platform. We evaluate our approach using a 6-DoF WidowX robotic arm (see Figure 2b). The 7D action space of the robot consists of 6D Cartesian end-effector motion, corresponding to relative changes in pose, as well as one dimension to control the opening and closing of the parallel jaw gripper. The state observations consist of the joint angles and RGB images from an overhead camera, which are 48×48 in simulation and either 64×64 or 128×128 in the real world.

Evaluation tasks. To effectively leverage data from prior tasks to solve new tasks, the prior tasks must share structural similarity with the new tasks. In our evaluation, we study a variety of pick and place tasks, where the shared structure is that each task involves picking up an object and placing it into or on top of some container or object, and the variability between the tasks corresponds to different containers or placement targets, different objects to be picked, and potentially even additional manipulations that must be performed on the container (e.g., opening a drawer prior to putting something inside). The tasks are performed in one of two scenes: a simpler scene where the objects and containers are in a tray, and a more visually complex kitchen scene. Both scenes contain distractor objects that are not involved in the tasks, and the robot is required to correctly learn which object to interact with, how to pick it, and where to place it. All tasks have sparse rewards evaluated using a simple hand-designed vision system, with a reward of +1 if the robot completes the forward (or backward) task, and 0 otherwise. While such rewards are easy to define, they present a substantial challenge for RL.

The test tasks that we fine-tune on, some of which are shown in Fig. 2b, span a range of difficulties and consist of picking and placing with objects and containers that were not seen in the prior data. Three of the tasks are in-distribution and hence similar to the prior data: placing a toy tiger in a drawer (which requires also opening the drawer, then closing it again to reset), placing a toy elephant in a pot, and placing a toy tiger on a lid. The other four tasks are out-of-distribution: placing a cup on a saucer, inserting a ring onto a peg, sorting a block into its correct slot, and moving a pot to the stove. The cup, ring, and pot require significantly different grasping behaviors than the objects seen in the prior data since they must be grasped from the edge. Additionally, successfully placing the ring on the peg and the block in the slot requires greater precision than any of the prior tasks.

Generating prior data. Our system can use prior data from any reasonable source, including demonstrations and prior RL runs, but for simplicity and consistency we employ a simple scripted policy to collect data for placing a wide variety of objects into containers (see Fig. 2). This provides a largely autonomous strategy to collect mediocre data for many objects. While this scripted policy fails very frequently, offline RL can make use of such mediocre data effectively to pretrain value functions and policies for downstream fine-tuning. We provide further details of the data we generated in the Appendix.

Providing demonstrations. In the transfer with demonstrations setting, we augment the scripted data with around 40 demonstrations of the target task collected by teleoperation with a 3DConnexion SpaceMouse Compact. Rewards are specified by a query at the end of each trajectory. This system allows specification of new tasks with no additional engineering effort.

Online training setup. Online training includes infrequent resets, to address the case where an object becomes stuck in a hard-to-reach (or unreachable) part of the workspace, but otherwise requires the robot to train autonomously. The resets are provided every 80 trials in simulation (about every hour), and roughly every 20-30 trials (about every 20-30 minutes) in the real world.

6 Experimental Results

Our experiments aim to evaluate the hypothesis that leveraging prior data from other tasks can simultaneously address multiple challenges in autonomous real-world robotic RL. To this end, we evaluate ARIEL on seven real-world downstream tasks and a suite of simulated robotic manipulation tasks. Our goal is to answer the following questions: (1) Does leveraging prior data enable mostly autonomous learning of both in-distribution and out-of-distribution tasks in the real-world? (2) Does ARIEL produce policies that better generalize to new conditions? (3) How does ARIEL compare to prior methods for learning with minimal resets that do not use prior data? (4) Does leveraging prior data via ARIEL lead to gains in sample-efficiency for a new task? Videos of the experiments can be found on the project website: <https://sites.google.com/view/ariel-berkeley/>

6.1 Evaluating ARIEL in the Real World

We first evaluate the performance of ARIEL when training online to solve new instances of the pick and place tasks in the real world. After pretraining on the datasets discussed in Section 5, we evaluate ARIEL on both in-distribution and out-of-distribution tasks using the direct transfer and transfer with demonstrations settings, respectively. We evaluate success rates of the policy learned

	Task	Offline Only	100 Trials	600 Trials	Only Demos
Direct Transfer	Put Tiger in Drawer	2/10	4/10	9/10	N/A
	Put Elephant in Pot	1/10	2/10	7/10	N/A
	Put Tiger on Lid	0/10	4/10	7/10	N/A
Transfer with Demos	Put Cup on Saucer	7/10	9/10	-	0/10
	Insert Ring onto Peg	4/10	10/10	-	0/10
	Put Block in Slot	5/10	8/10	-	0/10
	Move Pot to Stove	2/10	9/10	-	2/10

Table 1: **Real-world evaluation of the forward controller.** Fine-tuning is mostly autonomous with a reset every 20-30 trials. The first 3 tasks are in-distribution and use the direct transfer setting. The next 4 tasks are out-of-distribution and use the transfer with demonstrations setting.

in the offline phase, the policy learned after 100 trials (1.5 hours) of online training, and the final policy after 600 trials (9 hours).

Autonomous fine-tuning with infrequent resets with ARIEL significantly improves real-world performance. Table 1 shows the success rate of the forward controller for both the in-distribution and out-of-distribution tasks increases moderately after 100 trials (e.g., from 2/10 to 4/10 on *put tiger in drawer*) and substantially by the end of online training (e.g., from 4/10 to **9/10**). This indicates that ARIEL successfully optimizes the embeddings and policy parameters, with minimal resets, to perform the new task. Similar results for the performance of the backward controller are included in the Appendix. Notably, fine-tuning from only the small set of demonstrations (for the out-of-distribution tasks) largely fails, meaning that the agent is successfully transferring skills from the other tasks in the prior data. Additionally, the autonomous fine-tuning phase does not simply robustify the previously seen behaviors, but can also lead to the emergence of new behaviors. In the *insert ring onto peg* task, the fine-tuned reset policy also learned useful retrying behaviors, such as shifting the ring to a more favorable grasping position so that the peg would not obstruct the robot from taking off the ring, a behavior it did not exhibit from offline training alone. This is best seen in the [accompanying video](#).

Training on diverse prior data improves zero-shot generalization in the real world. Next, we investigate whether initializing from prior data provides ARIEL with more robust representations that generalize more effectively to new conditions without any further adaptation. To study this hypothesis, we additionally evaluate the fine-tuned policies for the *tiger on lid*, *ring on peg*, and *cup on saucer* tasks in a setting where we swap out the object (but keep the same container). We do not expect the policies to succeed consistently in this case, but we see in Table 2 that ARIEL policies exhibit some generalization, attaining an average success rate of **54%** at the best epoch. A baseline that uses only the data collected for each target task (i.e., either only *tiger on lid*, *ring on peg*, or *cup on saucer*) only succeeds in 12% of trials on the new objects. This suggests that pretraining on multi-task prior data does effectively boost generalization.

Interestingly, we observe that while fine-tuning improves the performance of ARIEL policies on the target tasks (see Table 1), fine-tuning on the target tasks adversely affects the zero-shot generalization performance on a new object. This is to be expected, since even though our online training procedure replays the prior data, we train with an increasing proportion of online data as online training goes on, making the policy more specialized to the target task. This observation is also consistent with prior RL works [39, 40] that note a drop in performance on test tasks as more updates are made on the training tasks. We anticipate that more principled early stopping or replay of the prior data could alleviate this issue, which is an interesting avenue for future work.

6.2 Evaluating ARIEL in Simulation

Lastly, we briefly present simulated experiments to compare ARIEL to prior autonomous learning approaches and ablations. Further details and analysis can be found in the Appendix.

ARIEL outperforms prior approaches for autonomous learning. We compare to R3L [6], which alternates between training a forward controller to optimize a task-completion reward and training a perturbation controller that optimizes a novelty exploration bonus. This method has been proposed specifically to handle reset-free learning for real-world RL problems. We also compare to an ablation (**Multi-task RL**) that does not optimize the task embeddings \mathbf{z}_f and \mathbf{z}_b over the course of

Target Task	Unseen Task	ARIEL by # Trials			Target Data Only
		100	360	600	Best Epoch
Put Tiger on Lid	Put Monkey on Lid	5/10	6/10	5/10	6/10
Put Tiger on Lid	Put Rabbit on Lid	2/10	4/10	0/10	0/10
Put Tiger on Lid	Put Hippo on Lid	3/10	5/10	0/10	0/10
Put Cup on Saucer	Put Orange Pot on Saucer	6/10	-	-	0/10
Insert Ring on Peg	Insert Black Ring on Peg	6/10	-	-	0/10

Table 2: **Generalization.** We evaluate the zero-shot generalization performance of policies fine-tuned with ARIEL. We take the policies obtained after online fine-tuning on the *tiger on lid*, *cup on saucer*, and *ring on peg* target tasks and evaluate them zero-shot on unseen tasks with interchanged objects. We compare with a baseline trained on only the data collected for the target tasks, without first training on the prior data (Target Data Only). We find that policies initialized by training on diverse prior data (ARIEL) generalize better to unseen tasks.

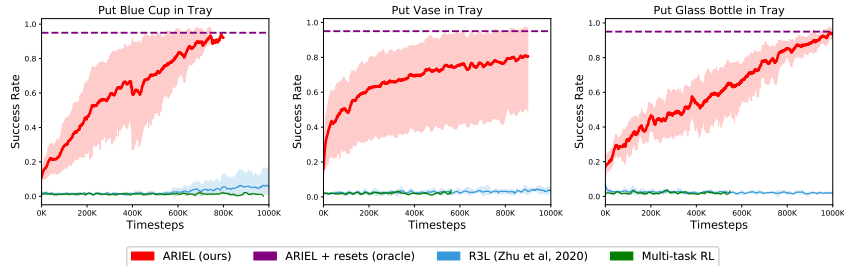


Figure 3: **Limited Resets.** Simulated domain experiments comparing our method to prior works in reset-free and multi-task learning. Ours is the only method that learns in this limited-reset setting.

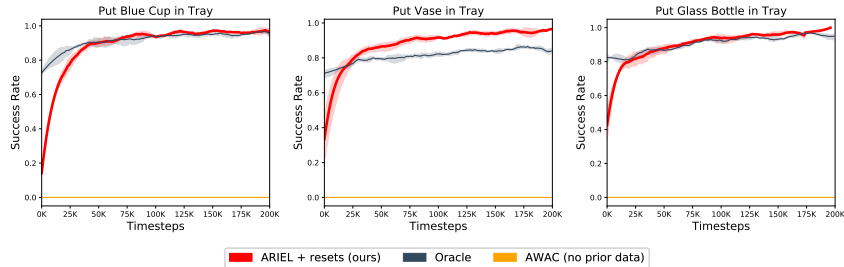


Figure 4: **Sample Efficiency.** Simulated domain experiments comparing our method to (1) an oracle with offline data for the downstream task, and (2) learning without any prior data. Unlike in Figure 3, these experiments had resets at the end of every episode. Our method adapts almost as quickly as the oracle approach, whereas RL from scratch fails to make any progress.

autonomous online fine-tuning, but instead fine-tunes the policy using a fixed task index (that was unused during pre-training). Finally, we compare to an “oracle” version of our approach, labeled **ARIEL + resets**, which assumes access to external resets at the end of each episode. Figure 3 shows that ARIEL and its oracle reset variant are the only methods that succeed at learning the new tasks, and the full ARIEL method closely matches the oracle.

ARIEL enables sample-efficient learning of the new task. Next, we compare our method to simply applying RL to the target task, using the same RL algorithm as our system (**AWAC (no prior data)**), as well as an **oracle** method which is trained offline on data coming from only the single new task of interest and then trained online on the same task. Perhaps unsurprisingly, we found that learning from scratch fails in the challenging setting of learning from images and sparse rewards. However, our method learns just as efficiently as the oracle despite only having access to offline data for other tasks and not the new task of interest. Thus, our method demonstrates that properly leveraging prior data can improve sample-efficiency even when data is only available for other tasks.

7 Discussion and Limitations

In this work, we proposed overcoming the numerous challenges of real-world robotic reinforcement learning through better leveraging prior datasets. While reinforcement learning often involves acquiring a skill from scratch, such a formalism is not well-suited to real world conditions where running online data collection is expensive, and previously collected datasets are often accessible. While the use of previously collected datasets for tackling a particular challenge (such as that of sample efficiency [1], or better generalization [41]) has been addressed in prior work, our work aims to address such challenges jointly in a single robotic learning system, which leverages prior data as the primary mechanism to facilitate autonomy during online training, improve efficiency, and boost generalization. In our experiments, we show that our method is able to make consistent progress in online fine-tuning despite having to learn from sparse rewards, matching or exceeding the final performance of an oracle baseline that receives prior data *of the actual test task*, and significantly outperforming a baseline without prior data. This supports our central hypothesis that prior data can be a significant facilitator for real-world robotic RL.

Limitations. The primary limitation of our approach is that our online target tasks are structurally quite similar to the prior data used for offline pretraining (particularly in the direct transfer setting). While the objects seen during online training are different, they do not require significantly distinct physical skills. We believe that increasing the diversity and breadth of the prior data will make the offline pretrained model useful for a broader range of new tasks. Exploring this direction by scaling up the proposed approach is an exciting avenue for future work.

Acknowledgments

This research was supported by the Office of Naval Research, NSF CAREER IIS-1651843, and ARO W911NF-21-1-0097, with computing support from Google.

References

- [1] A. Nair, M. Dalal, A. Gupta, and S. Levine. Accelerating online reinforcement learning with offline datasets. *arXiv preprint arXiv:2006.09359*, 2020.
- [2] D. Kalashnikov, J. Varley, Y. Chebotar, B. Swanson, R. Jonschkowski, C. Finn, S. Levine, and K. Hausman. Mt-opt: Continuous multi-task robotic reinforcement learning at scale. *arXiv preprint arXiv:2104.08212*, 2021.
- [3] K. Hausman, J. T. Springenberg, Z. Wang, N. Heess, and M. Riedmiller. Learning an embedding space for transferable robot skills. In *International Conference on Learning Representations*, 2018.
- [4] W. Han, S. Levine, and P. Abbeel. Learning compound multi-step controllers under unknown dynamics. In *2015 IEEE/RSJ International Conference on Intelligent Robots and Systems (IROS)*, pages 6435–6442. IEEE, 2015.
- [5] B. Eysenbach, S. Gu, J. Ibarz, and S. Levine. Leave no trace: Learning to reset for safe and autonomous reinforcement learning. *arXiv preprint arXiv:1711.06782*, 2017.
- [6] H. Zhu, J. Yu, A. Gupta, D. Shah, K. Hartikainen, A. Singh, V. Kumar, and S. Levine. The ingredients of real-world robotic reinforcement learning. *arXiv preprint arXiv:2004.12570*, 2020.
- [7] K. Xu, S. Verma, C. Finn, and S. Levine. Continual learning of control primitives: Skill discovery via reset-games. *arXiv preprint arXiv:2011.05286*, 2020.
- [8] A. Sharma, A. Gupta, S. Levine, K. Hausman, and C. Finn. Autonomous reinforcement learning via subgoal curricula. *Advances in Neural Information Processing Systems*, 34, 2021.
- [9] J. Peters and S. Schaal. Reinforcement learning by reward-weighted regression for operational space control. In *Proceedings of the 24th international conference on Machine learning*, pages 745–750, 2007.

- [10] D. Kalashnikov, A. Irpan, P. Pastor, J. Ibarz, A. Herzog, E. Jang, D. Quillen, E. Holly, M. Kalakrishnan, V. Vanhoucke, et al. Qt-opt: Scalable deep reinforcement learning for vision-based robotic manipulation. *arXiv preprint arXiv:1806.10293*, 2018.
- [11] Y. Wu, G. Tucker, and O. Nachum. Behavior regularized offline reinforcement learning. *arXiv preprint arXiv:1911.11361*, 2019.
- [12] S. Fujimoto, D. Meger, and D. Precup. Off-policy deep reinforcement learning without exploration. In *International Conference on Machine Learning*, pages 2052–2062. PMLR, 2019.
- [13] A. Kumar, J. Fu, G. Tucker, and S. Levine. Stabilizing off-policy q-learning via bootstrapping error reduction. *arXiv preprint arXiv:1906.00949*, 2019.
- [14] X. B. Peng, A. Kumar, G. Zhang, and S. Levine. Advantage-weighted regression: Simple and scalable off-policy reinforcement learning. *arXiv preprint arXiv:1910.00177*, 2019.
- [15] Z. Wang, A. Novikov, K. Zolna, J. T. Springenberg, S. Reed, B. Shahriari, N. Siegel, J. Merel, C. Gulcehre, N. Heess, et al. Critic regularized regression. *arXiv preprint arXiv:2006.15134*, 2020.
- [16] A. Kumar, A. Zhou, G. Tucker, and S. Levine. Conservative q-learning for offline reinforcement learning. *arXiv preprint arXiv:2006.04779*, 2020.
- [17] S. Fujimoto and S. S. Gu. A minimalist approach to offline reinforcement learning. *arXiv preprint arXiv:2106.06860*, 2021.
- [18] I. Kostrikov, R. Fergus, J. Tompson, and O. Nachum. Offline reinforcement learning with fisher divergence critic regularization. In *International Conference on Machine Learning*, pages 5774–5783. PMLR, 2021.
- [19] I. Kostrikov, A. Nair, and S. Levine. Offline reinforcement learning with implicit q-learning. 2021.
- [20] A. Wilson, A. Fern, S. Ray, and P. Tadepalli. Multi-task reinforcement learning: a hierarchical bayesian approach. In *Proceedings of the 24th international conference on Machine learning*, pages 1015–1022, 2007.
- [21] E. Parisotto, J. L. Ba, and R. Salakhutdinov. Actor-mimic: Deep multitask and transfer reinforcement learning. *arXiv preprint arXiv:1511.06342*, 2015.
- [22] Y. W. Teh, V. Bapst, W. M. Czarnecki, J. Quan, J. Kirkpatrick, R. Hadsell, N. Heess, and R. Pascanu. Distral: Robust multitask reinforcement learning. *arXiv preprint arXiv:1707.04175*, 2017.
- [23] L. Espeholt, H. Soyer, R. Munos, K. Simonyan, V. Mnih, T. Ward, Y. Doron, V. Firoiu, T. Harley, I. Dunning, et al. Impala: Scalable distributed deep-rl with importance weighted actor-learner architectures. In *International Conference on Machine Learning*, pages 1407–1416. PMLR, 2018.
- [24] M. Hessel, H. Soyer, L. Espeholt, W. Czarnecki, S. Schmitt, and H. van Hasselt. Multi-task deep reinforcement learning with popart. In *Proceedings of the AAAI Conference on Artificial Intelligence*, volume 33, pages 3796–3803, 2019.
- [25] T. Yu, S. Kumar, A. Gupta, S. Levine, K. Hausman, and C. Finn. Gradient surgery for multi-task learning. *arXiv preprint arXiv:2001.06782*, 2020.
- [26] Z. Xu, K. Wu, Z. Che, J. Tang, and J. Ye. Knowledge transfer in multi-task deep reinforcement learning for continuous control. *arXiv preprint arXiv:2010.07494*, 2020.
- [27] R. Yang, H. Xu, Y. Wu, and X. Wang. Multi-task reinforcement learning with soft modularization. *arXiv preprint arXiv:2003.13661*, 2020.
- [28] S. Sodhani, A. Zhang, and J. Pineau. Multi-task reinforcement learning with context-based representations. *arXiv preprint arXiv:2102.06177*, 2021.

- [29] T. Yu, A. Kumar, Y. Chebotar, K. Hausman, S. Levine, and C. Finn. Conservative data sharing for multi-task offline reinforcement learning. *Advances in Neural Information Processing Systems*, 34, 2021.
- [30] A. Sharma, K. Xu, N. Sardana, A. Gupta, K. Hausman, S. Levine, and C. Finn. Autonomous reinforcement learning: Formalism and benchmarking. *arXiv preprint arXiv:2112.09605*, 2021.
- [31] A. Gupta, J. Yu, T. Z. Zhao, V. Kumar, A. Rovinsky, K. Xu, T. Devlin, and S. Levine. Reset-free reinforcement learning via multi-task learning: Learning dexterous manipulation behaviors without human intervention. *arXiv preprint arXiv:2104.11203*, 2021.
- [32] K. Lu, A. Grover, P. Abbeel, and I. Mordatch. Reset-free lifelong learning with skill-space planning. *arXiv preprint arXiv:2012.03548*, 2020.
- [33] S. Ha, P. Xu, Z. Tan, S. Levine, and J. Tan. Learning to walk in the real world with minimal human effort. *arXiv preprint arXiv:2002.08550*, 2020.
- [34] A. Gupta, C. Lynch, B. Kinman, G. Peake, S. Levine, and K. Hausman. Bootstrapped autonomous practicing via multi-task reinforcement learning. *arXiv preprint arXiv:2203.15755*, 2022.
- [35] T. P. Lillicrap, J. J. Hunt, A. Pritzel, N. Heess, T. Erez, Y. Tassa, D. Silver, and D. Wierstra. Continuous control with deep reinforcement learning. *arXiv preprint arXiv:1509.02971*, 2015.
- [36] T. Haarnoja, A. Zhou, P. Abbeel, and S. Levine. Soft actor-critic: Off-policy maximum entropy deep reinforcement learning with a stochastic actor. In *International conference on machine learning*, pages 1861–1870. PMLR, 2018.
- [37] K. Rakelly, A. Zhou, C. Finn, S. Levine, and D. Quillen. Efficient off-policy meta-reinforcement learning via probabilistic context variables. In *International conference on machine learning*, pages 5331–5340. PMLR, 2019.
- [38] R. Rubinstein. The cross-entropy method for combinatorial and continuous optimization. *Methodology and computing in applied probability*, 1(2):127–190, 1999.
- [39] K. Cobbe, C. Hesse, J. Hilton, and J. Schulman. Leveraging procedural generation to benchmark reinforcement learning. In *International conference on machine learning*, pages 2048–2056. PMLR, 2020.
- [40] D. Ghosh, J. Rahme, A. Kumar, A. Zhang, R. P. Adams, and S. Levine. Why generalization in rl is difficult: Epistemic pomdps and implicit partial observability. *Advances in Neural Information Processing Systems*, 34, 2021.
- [41] Y. Lin, A. Zeng, S. Song, P. Isola, and T. Lin. Learning to see before learning to act: Visual pre-training for manipulation. *CoRR*, abs/2107.00646, 2021.
- [42] E. Coumans and Y. Bai. Pybullet, a python module for physics simulation for games, robotics and machine learning. *GitHub repository*, 2016.
- [43] A. X. Chang, T. A. Funkhouser, L. J. Guibas, P. Hanrahan, Q. Huang, Z. Li, S. Savarese, M. Savva, S. Song, H. Su, J. Xiao, L. Yi, and F. Yu. Shapenet: An information-rich 3d model repository. *CoRR*, abs/1512.03012, 2015.

A Appendix

Videos of the experiments can be found on the project website: <https://sites.google.com/view/ariel-berkeley/>

A.1 Implementation Details and Hyperparameters

We choose advantage-weighted actor-critic (AWAC) as the underlying RL algorithm for both the online and offline phases of ARIEL and all comparison methods because it addresses the specific challenges that arise when learning behaviors offline and then fine-tuning them online [1]. AWAC is an actor-critic method that alternates between a policy evaluation phase (Equation 1), where it trains a parametric Q-function, $Q_\phi(\mathbf{s}, \mathbf{a})$, to minimize the error between two sides of the Bellman equation on the samples from the offline dataset, and a policy improvement phase (Equation 2) where it improves a parametric policy $\pi_\theta(\mathbf{a}|\mathbf{s})$ via advantage-weighted updates. Advantage-weighted updates perform policy improvement by cloning actions that are highly advantageous under the learned Q-function and are hence, more likely to improve upon the data-collection policy. Denoting the offline dataset as $\mathcal{D} = \{(\mathbf{s}_i, \mathbf{a}_i, \mathbf{s}'_i, r_i)\}_{i=1}^N$, where $(\mathbf{s}_i, \mathbf{a}_i, \mathbf{s}'_i, r_i)$ denotes a single transition, the training objectives for AWAC are given by:

$$\hat{Q}_\phi^\pi \leftarrow \arg \min_{\phi} \mathbb{E}_{\mathbf{s}, \mathbf{a}, \mathbf{s}' \sim \mathcal{D}} [(Q_\phi(\mathbf{s}, \mathbf{a}) - (r + \gamma Q_\phi(\mathbf{s}', \mathbf{a}'))^2] \quad (1)$$

$$\hat{\pi} \leftarrow \arg \max_{\theta} \mathbb{E}_{\mathbf{s}, \mathbf{a} \sim \mathcal{D}} [\log \pi_\theta(\mathbf{a}|\mathbf{s}) \cdot \exp(\hat{A}^\pi(\mathbf{s}, \mathbf{a}))],$$

$$\text{where } \hat{A}^\pi(\mathbf{s}, \mathbf{a}) := \hat{Q}_\phi^\pi(\mathbf{s}, \mathbf{a}) - \mathbb{E}_{\mathbf{a}' \sim \pi} [\hat{Q}_\phi^\pi(\mathbf{s}, \mathbf{a}')] . \quad (2)$$

Our hyperparameters for AWAC are listed in Table 3. Notably, since AWAC is an off-policy RL algorithm, we have the option of continuing to train on the prior data during the online phase. We hypothesize that including the prior data during online adaptation prevents the agent from overfitting to the new task and improves generalization, so we continue to train on the prior data even during the online fine-tuning phase. As our goal is to make robotic learning as autonomous as possible, we use images observations as part of our input to the RL agent. Image observations allow our system to learn from a diverse range of different tasks without needing to hand-engineer state representations suitable for each task. Because we are learning from images we use convolutional neural networks to model the policy and Q-function. (see Figure 5 and Table 4). The observations additionally consist of the state of the robot’s joints, and the task embedding \mathbf{z} . Lastly, during the online phase the pose of the robot is moved to a neutral position at the beginning of every trial, since there is no physical limitation that prevents doing this automatically, but the robot must still handle the fact that the objects in the scene maintain their position across trials. We now provide further details specific to each method:

- **Multi-Task RL:** We modify the policy and Q function architectures to accept two additional one-hot task indices. These task indices go unused during offline learning, but we use them to label the new data during online training.
- **R3L:** For the RND networks we use the same CNN architecture as the policy and Q function networks but set the output dimension to 5.
- **Oracle:** We learn a single-task policy with a single-task dataset consisting of 512 trajectories collected in the same manner as the rest of the simulated data.
- **ARIEL:** For CEM, we use a Gaussian mixture model as the sampling distributions with a number of components equal to the number of tasks in the prior data. In simulation, we update the sampling distributions every 10 trajectories, fitting them to the $J = 25$ most recent successful task embeddings. In the real world domains, we update the sampling distributions every 10 trajectories, fitting them to the $J = 10$ most recent successful task embeddings.

A.2 Real-World Experiments

In this section, we provide additional details on our real world experiments, the results for which were presented in Section 6.1. We utilize 3 different robotic setups for our experiments (Figure

Hyperparameter	Value
Target Network Update Frequency	1 step
Discount Factor γ	0.9666
Beta	0.01
Batch Size	64
Meta Batch Size	8
Soft Target τ	$5e^{-3}$
Policy Learning Rate	$3e^{-4}$
Q Function Learning Rate	$3e^{-4}$
Reward Scale	1.0
Alpha	0.0
Policy Weight Decay	$1e^{-4}$
Clip Score	0.5

Table 3: Hyperparameters for AWAC

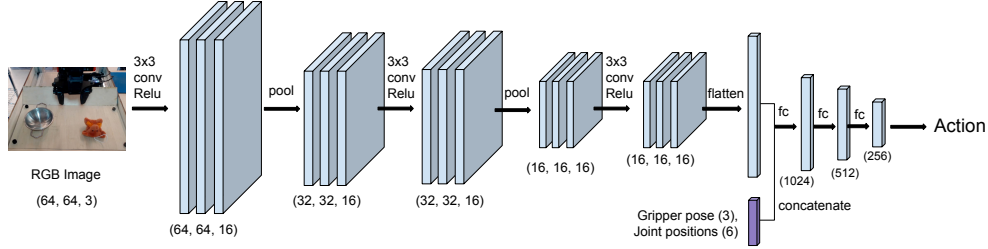


Figure 5: **CNN architecture we use for our policy and Q-function.** Our method learns robotic manipulation skills from raw image inputs. Here we show the architecture for the policy. For our Q-functions, we additionally concatenate the action along with the gripper pose and joint positions and set the output dimension to 1.

Attribute	Value
Input Width	48/64/128
Input Height	48/64/128
Input Channels	3
Kernel Sizes	[3, 3, 3]
Number of Channels	[16, 16, 16]
Strides	[1, 1, 1]
Fully Connected Layers	[1024, 512, 256]
Paddings	[1, 1, 1]
Pool Type	Max 2D
Pool Sizes	[2, 2, 1]
Pool Strides	[2, 2, 1]
Pool Paddings	[0, 0, 0]
Image Augmentation	Random Crops
Image Augmentation Padding	4

Table 4: CNN architecture for policy and Q-function networks. We use 48x48 images in simulation, 64x64 images in the **Tray Container** and **Tray Drawer** scenes, and 128x128 images in the **Kitchen** scene, however the rest of the architecture is the same across experiments.

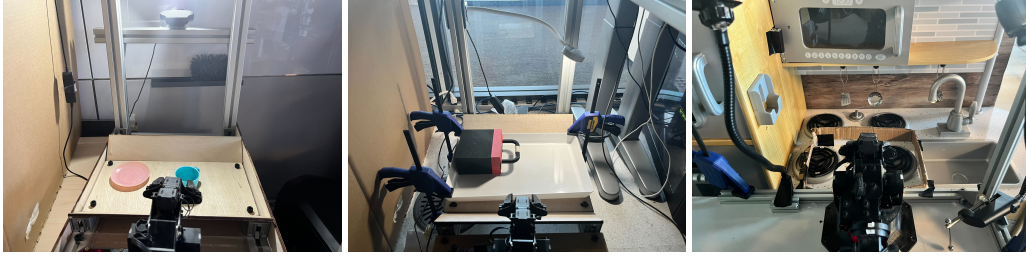


Figure 6: Robotic environments for real-world experiments

6). The first, denoted **Tray Container**, consists of a simple tray with objects and one of multiple containers. The second, denoted **Tray Drawer**, consists of a tray with objects and a 3D-printed drawer. The third, denoted **Kitchen**, is a toy kitchen to showcase the performance of the method under greater visual diversity.

A.2.1 Real-World Dataset Details

The real-robot dataset consists of picking and placing a variety of objects, including stuffed animals, rigid shapes, and toys, into a variety of containers, including plates, pots, baskets, and drawers. We utilize scripted policies in order to collect a large amount of data interacting with these objects. Since the prior dataset needs to initialize both the forward and backward directions for new tasks, we perform scripted collection in a reset-free manner, with the robot attempting to move the objects both into and out of containers. The **Tray Container** and **Kitchen** environments contain distractor objects that are not involved in the tasks so the robot is required to pay attention to the task embedding z to determine which object to interact with. In Table 5 we provide details on number of tasks, number of trajectories, and other dataset properties.

Attribute	Tray Container	Tray Drawer	Kitchen
Timesteps per Offline Trajectory	15	30	25
Timesteps per Online Trajectory	20	35	25
Forward Tasks	20	4	10
Backward Tasks	20	4	10
Number of Trajectories Per Task	500	150	50
Average Success Rate	0.35	0.93	0.47

Table 5: Real-world data details for the **Tray Container**, **Tray Drawer**, and **Kitchen** scenes.

A.2.2 Backward Controller Performance

In Table 6 we provide additional evaluation of the backward controller for the **Tray Container** and **Tray Drawer** scenes. We find that the performance of the backward controller improves throughout online training similar to the forward controller.

Task	Offline Only	100 Trials	600 Trials
Put Tiger in Drawer	5/10	6/10	7/10
Put Elephant in Pot	1/10	8/10	10/10
Put Tiger on Lid	2/10	6/10	6/10

Table 6: Real-world evaluation of the backward controller in the **Tray Container** and **Tray Drawer** scenes. These tasks use the direct transfer setting. Fine-tuning is mostly autonomous with a reset every 20-30 trials.

Target Task	Unseen Task	ARIEL by # Trials			Target Data Only
		100	360	600	Best Epoch
Put Tiger in Drawer	Put Pickle in Drawer	3/5	5/5	3/5	1/5
Put Tiger in Drawer	Put Turtle in Drawer	1/5	4/5	2/5	2/5
Put Tiger in Drawer	Put Dog in Drawer	2/5	2/5	4/5	2/5

Table 7: **Generalization.** We compare the zero-shot generalization performance on unseen objects of ARIEL and a baseline in the **Tray Drawer** scene. A policy pretrained on multi-task prior data and fine-tuned on the *put tiger in drawer* task (ARIEL) generalizes better than a policy trained on only *put tiger in drawer* data (Target Data Only).



Figure 7: Objects used in zero-shot generalization experiments.

A.2.3 Further Generalization Results

In Table 7 we provide further zero-shot generalization results for the **Tray Drawer** scene. As shown in the main paper, a policy trained on multi-task prior data and fine-tuned on a target task (ARIEL) generalizes to unseen objects better than a policy trained on only target task data (Target Data Only). We evaluate the zero-shot generalization capabilities of the ARIEL policies at different stages during the process of fine-tuning on the target task (*put tiger in drawer*). As in the main paper, ARIEL policies at earlier stages of fine-tuning (360 vs 600 trials) demonstrate better zero-shot generalization capabilities to unseen objects than at later stages. Even if policy is initialized by training on diverse multi-task prior data, as more updates are made on the target task, the policy becomes more specialized and less capable of performing the unseen tasks.

A.2.4 Generalization Test Objects

The objects we use to test the zero-shot generalization capabilities of ARIEL are depicted in Figure 7. Note that although the objects chosen to test generalization in the **Tray Drawer** scene are seen in the prior data for the **Tray Container** scene, they are not contained in the prior data for the **Tray Drawer** scene.

A.3 Simulated Experiments

In this section, we provide additional details on our simulation experiments, the results for which were presented in Section 6.2. We utilize a Pybullet-based simulation [42] with a simulated version of the WidowX robot we use in the real world. The tasks also involve picking and placing objects and putting them into a container. We use 3D object models from the Shapenet dataset [43] to test our method on diverse objects. We utilize a near-convex decomposition of the models in order to maintain good contact physics. Figure 8 shows the simulated experiment setup.

We compare to two prior approaches in our simulated experiments. To evaluate how well our method enables learning with minimal resets, we compare to **R3L** [6], which alternates between training a forward controller to optimize a task-completion reward and training a perturbation controller that optimizes a novelty exploration bonus. We initialize the forward controller in R3L with the policy obtained by running offline multi-task RL on the prior data. We also compare to a method



Figure 8: (Left) The simulated experiment setup. (Right) Simulation training (upper) and test (lower) objects. Our offline prior dataset consists of only training objects.

Attribute	Value
Timesteps per Offline Trajectory	30
Timesteps per Online Trajectory	40
Forward Tasks	8
Backward Tasks	8
Number of Trajectories Per Task	512
Average Success Rate	0.38

Table 8: Simulated tasks prior data details.

that does *not* optimize the task embeddings \mathbf{z}_f and \mathbf{z}_b over the course of autonomous online fine-tuning. We refer to this approach as **Multi-task RL**. This is equivalent to first running multi-task offline RL on the prior dataset, and then fine-tuning the policy using a fixed task index (that was unused during pre-training) in an online phase afterwards. This method is conceptually similar to MT-Opt [2], but adapted to our pre-training and then fine-tuning setup, as opposed to the re-training from scratch approach followed by Kalashnikov et al. [2]. For instructive purposes, we also compare to an “oracle” version of our approach, labeled (**ARIEL + resets**), which assumes access to external resets at the end of each episode. While resetting every episode is prohibitively expensive in the real-world, we can still run this method in simulation for our understanding.

The results in Figure 3 show that ARIEL and its oracle reset variant are the only methods that succeed at learning the new tasks, and the full ARIEL method closely matches final oracle performance. While the poor performance of prior methods might be surprising, recall that these tasks require using raw image observations and sparse 0/1 rewards, which present a significant challenge for any RL approach. While **R3L** and **Multi-Task RL** both succeeded at learning the tasks in the offline phase (see Figure 9), they are unable to make progress during online training of the new task. The comparison to **Multi-task RL** indicates the importance of adapting the task embeddings: if the task embeddings are not adapted to the new task, distributional shift in the task embeddings may severely hamper effective reset-free learning.

A.3.1 Simulation Dataset Details

Just as in our real world experiments, we perform scripted collection in a reset-free manner, with the robot attempting to move the objects both into and out of the container. In Figure 8, we show the set of training and testing objects used in the various pick and place tasks. In Table 8 we provide details on number of tasks, number of trajectories and other dataset properties.

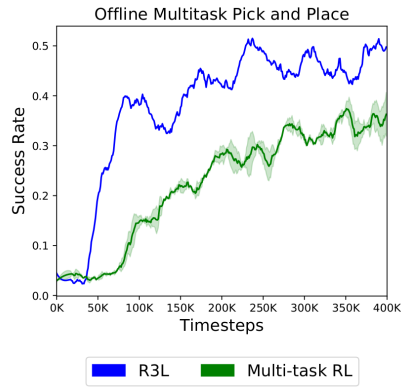


Figure 9: We see that the **R3L** and **Multi-task RL** baselines show a significant amount of learning in the offline stage, even though they perform poorly during fine-tuning as seen in Figure 3.